Evaluation of the influence of low pressure additive manufacturing processing conditions on printed polymer parts

Heather J. O'Connor*, Denis P. Dowling

School of Mechanical and Materials Engineering, University College Dublin, Belfield, Dublin 4, Ireland

*** Correspondence:** Email: heather.oconnor@ucdconnect.ie

Abstract

The properties of 3-D printed polymeric parts depend significantly on the processing conditions under which they are fabricated. This study aims to determine how the use of low-pressure additive manufacturing (AM) processing conditions, influences the mechanical performance of printed polymeric parts. This polymer material extrusion (PME) study was carried out using an open-source desktop printer, under both low pressure (1 Pa) and at atmospheric pressure. The printing study was carried out using acrylonitrile butadiene styrene (ABS), polylactic acid (PLA) and a nylon co-polymer (PA6). The resultant polymer parts were compared based on their printed mass, density, volume, porosity, surface energy, ATR-IR analysis and thermal properties (DSC). As expected only minor differences in chemical functionality were observed between parts printed under the two processing pressures. Under low-pressure printing conditions, the polymer parts exhibited some physical changes, when compared to those, printed under atmospheric conditions, such as an increase in density and a decrease in porosity. This was observed in particular with the low-pressure printing of PA6 parts, which exhibited an increase in density from 1.095 to 1.113 g / cm^3 and a decrease in porosity by 8%. Comparing low-pressure printed type V dog bones (ASTM D-638), with those printed at atmospheric pressure, it was observed that the ABS, PLA and PA6 exhibited an increase in Ultimate Tensile Strength of 9%, 13% and 42% respectively. It is proposed that the superior mechanical properties obtained for polymers printed under low pressure conditions, may be due to a combination of two factors. These are the reduction in porosity of the printed part and the reduction in heat loss at the printed polymer surface, yielding enhanced bonding between the polymer layers. In a further printing study carried out at atmospheric pressure in a nitrogen atmosphere, it was also demonstrated that any oxidation of the polymer layers during printing, did not significantly influence the mechanical properties of the resultant printed parts.

Keywords: Material Extrusion, Low Pressure, Vacuum Chamber, Tensile Strength

---

1. Introduction

Additive Manufacturing (AM) is a manufacturing process that fabricates parts, layer by layer, from a computer aided design [1]. It encompasses a range of techniques, such as binder jetting, direct metal laser sintering, stereolithography and Material Extrusion. AM holds many advantages over traditional manufacturing methods, primarily the ability to fabricate complex geometries, which dramatically shortens the design to production cycle.

Polymer material extrusion (PME) is one of the most widely used AM technologies and has been previously referred to by names such as fused filament fabrication (FFF) and the Stratasys trade-marked name, fused deposition modelling (FDM) [1]. In this process, a polymer filament is melted and extruded through a nozzle to create a cross section of the required part and each subsequent layer is fused onto the previous one until the part is complete [2]. The fusion of each polymer layer, occurs due to the formation of bonds along the polymer interface, driven by the thermal energy of the extruded material, which will ultimately determine the mechanical properties of the print. Therefore the temperature of the extruded polymer and the temperature of the interface of the deposited polymer layers both play an important role in determining the bond quality and overall print characteristics [3]. Several other processing parameters are crucial in determining the dimensional accuracy and the overall quality of the printed part [3-6]. For example, a number of authors have investigated the influence of layer thickness, 'road' width and air gap on the surface finish of printed ABS [4]. It was concluded that decreasing layer thickness increased the surface quality and dimensional accuracy. Furthermore, layer thickness has been correlated to the tensile strength of printed polymeric parts [7, 8]. It was observed that the strength of printed specimen first decreases then increases as the layer thickness is increased, due to thermal diffusion properties [8]. Several authors have also highlighted the importance of process parameters, such as layer orientation and the shell perimeter on the mechanical performance [7, 9, 10]. Tensile strength has been shown to depend heavily on the orientation of the deposited polymer. For example, studies carried out with ABS, compared strengths with a raster orientation of 0° (to the direction of tensile force) with specimen printed at a 90° orientation [9, 10]. These two studies demonstrated that, the former orientation exhibited superior mechanical strength. Ziemian et al. [9] demonstrated that when the layers were 0° to the force, the tensile strengths were 93% of those obtained for injection moulded parts. In contrast, when the layers were orientated at 90° to the force, the strengths were only 34% of those obtained for the injection moulded parts. Tanikella et al. [11] reported that the tensile strength of PME printed parts is dependent on their mass. They proposed a two-step process to predict mechanical strength, by examining the exterior of the printed part and then measuring the mass. This mass is compared to the theoretical value using densities for the material and the volume of the object. Higher print strength is directly correlated with higher print density.

The focus of the present study is to investigate both how a low-pressure environment during printing, as well as the absence of oxygen (by printing under a nitrogen atmosphere) influences the properties of the printed parts, via PME. To the authors knowledge, the investigation of the effect of low pressure on the resultant printed polymer part performance has not previously been reported. There have however been a small number of studies to investigate the influence of AM printing atmosphere on the properties of the resultant polymer parts. Lederle et al. [12] evaluated the printing of ABS via PME and a nylon co-polymer in a glove box under N_2. They reported that the resultant polymer part exhibited improved mechanical performance, with a 20% increase in the elongation at break obtained for ABS, while for Nylon, the tensile strength was improved by almost 30%. It was proposed that by printing in the absence of oxygen, that oxidation processes were suppressed, thus leading to a better layer adhesion.

This study focuses on the PME printing process. A comparison was carried out, between printing under reduced pressure (1 Pa) and at atmospheric pressure, on the properties of the thermoplastic polymers: acrylonitrile butadiene styrene (ABS), polylactic acid (PLA) and a polyamide 6 co-polymer blend (PA6). A further investigation was carried out with the PA6 only, to evaluate the influence of nitrogen only printing environment at atmospheric pressure, on the properties of the printed polymer parts.

2. Experimental Methods

This study was carried out using filaments of ABS (light blue, REAL-filament), PLA (white, REAL-filament) and a transparent PA6 blend (Markforged™). The ABS and PLA filament reels were stored in a desiccator prior to use and the PA6 was kept in a dry box (Pelican case supplied by Markforged™). The additive manufacturing was carried out inside a steel vacuum chamber (Figure 1), with internal diameter of 45 cm and height of 50 cm, operating either at atmospheric pressure or under low pressure. In the case of the latter the chamber was pumped using a rotary and roots blower pumping system and the pressure during printing was maintained at 1 Pa. Chamber pressure was monitored using an Edwards Active Gauge Controller. The PME printing studies were carried out using a Monoprice Select Mini 3D Printer V1 system (Figure 1). This printer was chosen based on its dimensions of 343 x 287 x 190 mm, with a build area of 120 x 120 x 120 mm, which allowed it to fit inside the vacuum chamber. When printing under N_2, the chamber was pumped down to a base pressure of 1 Pa, the pump line was shut-off and nitrogen was introduced and the chamber backfilled with the gas to allow it to return to atmospheric pressure.

Figure 1: Vacuum chamber (left) in which the PME printing studies were carried out using the MP Select Monoprice printer (right)

Cura 15.04.6 [13] was used to slice the STL file into a gcode and a micro SD card was used to load the gcode file on the printer. The print start time was delayed by 120 seconds to allow the chamber to be evacuated, before it began to print. For density and morphology measurements, square coupons 16 × 16 × 2 mm were printed using the PME system. For tensile testing, the type V specimen geometry was used (Figure 2), according to the ASTM D-638.

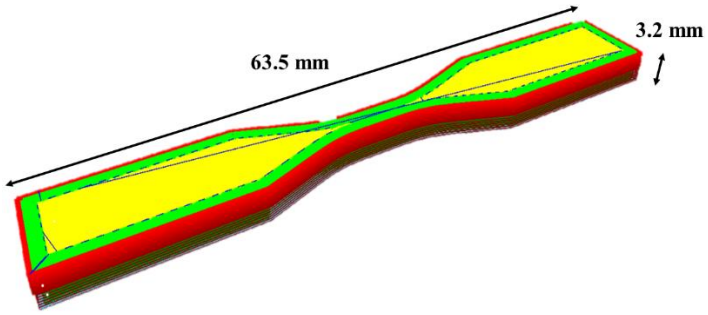

Figure 2: 3D schematic of Type V tensile specimen with shell perimeter.

2.1 Process Parameters

Tensile tests were carried out according to ASTM D-638, type V specimen. Optimised print parameters were chosen in terms of tensile strength and are as follows: A layer height of 0.2 mm, a raster orientation of 45 /- 45°. A shell perimeter of 2 mm was chosen, which caused the fibres to be aligned at a 0° angle to the tensile force, as this has previously been shown to yield higher tensile strengths [14]. The fill density was at 100% and the infill overlap was at 15%. The nozzle diameter was 0.4 mm and the percentage flow of the filament was 100% at a print speed of 20 mm/s in the case of ABS and PA6 and 40 mm/s in the case of PLA. The print temperature of each polymer was based on the filament manufacturer's recommendations (Table 1). The parameters chosen for the tensile specimen were also used for the fabrication of the coupons.

Table 1: Nozzle and bed temperatures used for the PLA, ABS and PA6 filament.

Filament	Nozzle Temperature (°C)	Bed Temperature (°C)
PLA	215	40
ABS	250	80
PA6	250	80

2.2 Print Characterisation

The average width and thickness across each printed specimen was recorded using a digital vernier callipers, Digi Plus-Line supplied by Vogel Germany GmbH & Co.KG. Each printed specimen was weighed to four decimal places using a Sartorius MC1 Analytic AC 210 S balance and the density of each was calculated according to the Archimedes principle, using the suspension method as described by S.W. Hughes [15]. The specimen density, d_S, was calculated using the formula given in equation 1:

$$d_s = d_w \times \frac{m1}{m2}$$ Equation 1

Where d_w is the density of water, m_1 mass of the specimen in air and m_2 is the mass of the specimen, suspended and stationary in water, measured on the analytic balance, which equals the volume. Cross sections were observed via optical microscopy to measure the porosity of the coupons. The porosity was measured by converting the microscopy images into binary images. This allowed the ratio of voided area to total area to be calculated as a percentage. A minimum of nine images were used, three samples per polymer at both printing conditions and three images from each sample was obtained and averaged. Surface roughness measurements were carried out using a Wyko NT1100 optical profilometer in vertical scanning interferometer mode (VSI). This system was used to calculate the arithmetic average roughness R_a. The magnification used was 50 X. The roughness of a single track - taken from the shell perimeter, with a sample size of 91.3 × 120 µm, was obtained per polymer in order to compare layers printed under both low pressure and atmospheric printing conditions. Each measurement per sample was taken five times and averaged. The print quality was also examined using a VHX- 5000 Keyence Microscope and an Olympus Gx51 Inverted Metallurgical Microscope and a Tabletop Hitachi tm 1000 SEM.

Differential scanning calorimetry (DSC) was used to compare the polymer glass transition temperatures and the percentage crystallinity. DSC measurements were performed on ABS, PLA and PA6 using a Netzsch DSC214, under a 40 mm/min nitrogen atmosphere and a heating rate of 10 K min^{-1}. In the case of ABS, the polymer was heated to 200°C, cooled back to -140°C and this was repeated for the second heating. PLA was heated to 200°C, cooled back to 0°C and this was repeated for the second heating. PA6 was heated to 300°C, cooled to -20°C and this process was again repeated. The glass transition temperature was evaluated according to the half-step method. The percentage crystallinity, $X_{m,}$ was calculated using equation 2 [16], where the enthalpy of fusion, ΔH_m, was obtained from integrating the melting peak. The post crystallisation peak (only present in PLA) was integrated to calculate ΔH_A and the heat of fusion of 100% crystalline PLA and PA6, ΔH_m^0 , were taken as 93 and 176 J g^{-1} respectively [17] [18]. Analysis of the peaks was performed using Proteus evaluation software.

$$X_m = \left(\frac{\Delta H_m - \Delta H_A}{\Delta H_m^0}\right) \times 100$$ Equation 2

FT-IR spectra of the printed polymers were obtained using a Nicolet iS50 FTIR Spectrometer, Wavenumber range: 8000-650 cm-1, diamond ATR. To avoid contamination and interference from

degradation of the printed polymers on the spectra, the specimen was sliced open and the freshly cut side was used for measurements. Surface energy measurements were carried out on an OCA 20 Dataphysics Instrument using the Owens, Wendt, Rabel and Kaelble technique (OWRK) and deionised water, diiodomethane and ethylene glycol as test liquids [19].

2.3 Mechanical Performance

Tensile tests were obtained in accordance with ASTM D-638 [20], these were completed in order to determine the mean ultimate tensile strength for each of the polymer samples printed under both atmospheric and low-pressure printing conditions. A total of 15 specimens (type V) were tested for each polymer at each condition. Tensile tests were performed on a Zwick Roell z005 universal tester (10kN load cell), with a video extensometer at a rate of 1 mm / minute for PLA and ABS and 10 mm / minute for PA6. The tensile modulus was calculated by finding the slope of the stress strain curve between the strain of 0.02 – 0.2.

3. Results and Discussion

3.1 Physical Print Characterisation

The three polymers, ABS, PLA and PA6 were printed under both atmospheric and low-pressure conditions, as described in the previous section. The resultant polymer coupons were compared in terms of print quality and chemical functionality. Coupons printed under low pressure, exhibited a higher surface finish, with the individual print tracks being less defined (Figure 3 and 4). The microscopy images given in Figure 4, for the ABS polymer printed at atmospheric pressure and low pressure, would indicate more rapid cooling in the case of the former based on the lack of 'merging' between the filaments as they are laid down. A similar effect was observed for the two other polymers evaluated.

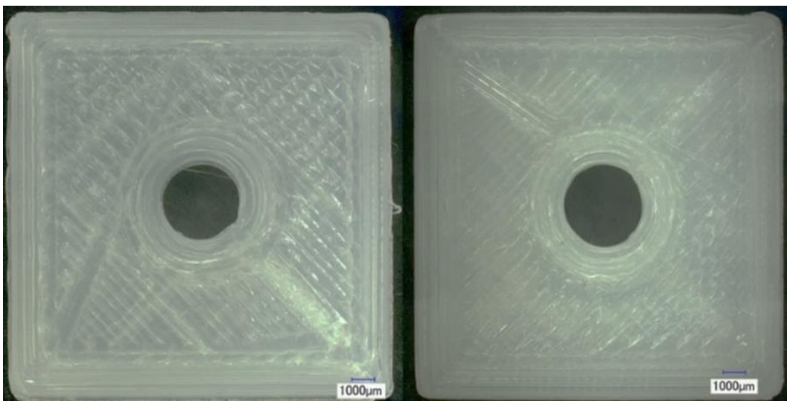

Figure 3: PA6 printed coupons, printed under atmospheric conditions (left) and under low pressure (right).

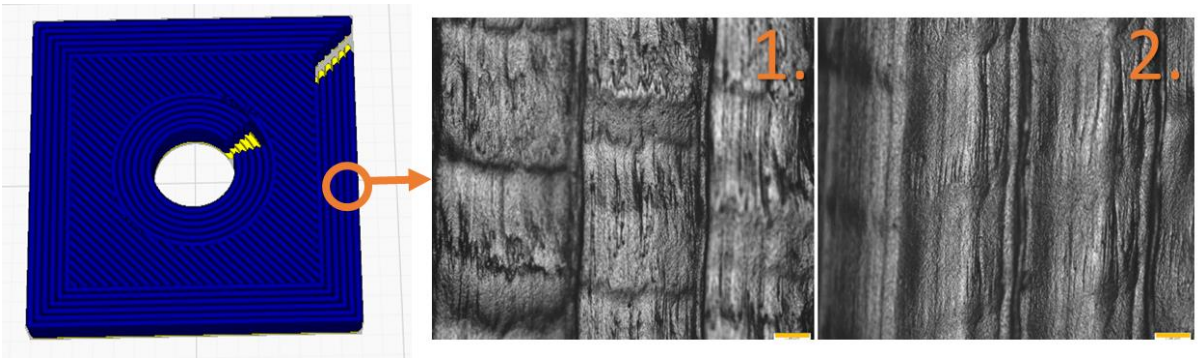

Figure 4: Optical microscopy images comparing the morphology of the surface tracks of ABS printed under both (1.) atmospheric and (2.) low-pressure conditions. Scale bar: 100 µm

The printed coupons were gold-coated and their morphology and roughness examined using optical profilometry. The ABS printed specimens exhibited a more homogeneous morphology, when printed under low pressure conditions. As outlined above, this is due to the individual tracks merging into each other. As seen in Figure 5, the average R_a value for the ABS and PLA polymers decreased when printed under low pressure. The PA6 printed parts had the lowest average R_a value and exhibited a minor increase when printed under low-pressure. It can be observed in the error bars that the standard deviation in roughness values obtained, decreased in the following order: ABS > PLA > PA6.

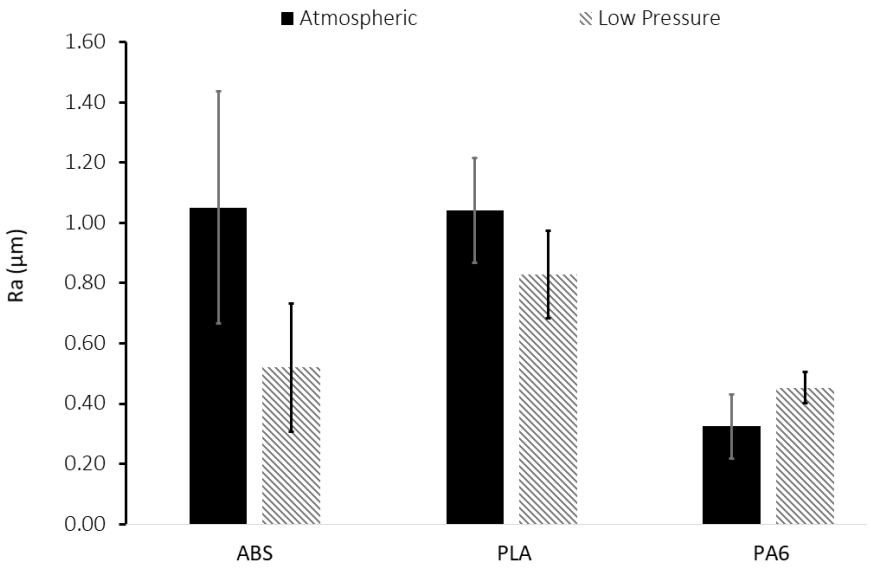

Figure 5: Roughness (R_a) values obtained for the printed polymers under both low and atmospheric pressure conditions.

Table 2 provides information on the mass, volume, density and porosity of the printed polymers. The density of ABS, PLA and PA6 filament is reported as 1.04 g/cm^3 [21], 1.24 g/cm^3 [22] and 1.10 g/cm^3 [23] respectively. In the case of all three polymers, the average weight, volume and density of the printed coupon increased when printed under low-pressure. The largest increase in density was observed for the PA6. This observed increase in mass and volume and reduction in porosity of the printed parts is likely to be due to the change in thermal gradient when printing under low pressure. As the polymers are extruded at 1 Pa, the filament cools more slowly and thus may remain above its glass transition temperature during deposition. This thermal effect of the low-pressure printing can be described as follows: During the PME deposition process under standard atmospheric conditions, heat is dissipated by conduction and forced convection. The resulting reduction in temperature, from these processes, causes the material to quickly solidify onto the previous layer [6]. In contrast with vacuum processing,

heat is largely dissipated by conduction. The reduced heat loss may enable the polymer to remain in a semi-liquid state as the layers are being deposited, thus facilitating the 'merging' of the printed layers.

Table 2: Comparison of mass, volume, density and porosity under both atmospheric and low-pressure printing conditions.

Polymer / Pressure	Weight (g)	Volume (cm^3)	Density (g / cm^3)	Porosity (%)
ABS / Atmospheric	0.5080 ± 0.0001	0.5060 ± 0.0004	1.0039 ± 0.0007	10.8 ± 4.2
ABS / Low	0.5150 ± 0.0050	0.5109 ± 0.0048	1.0079 ± 0.0004	4.8 ± 2.1
PLA / Atmospheric	0.5547 ± 0.0168	0.5543 ± 0.0158	1.0183 ± 0.0014	15.5 ± 4.9
PLA / Low	0.6115 ± 0.0014	0.6108 ± 0.0007	1.0195 ± 0.0031	8.1 ± 4.2
PA6 / Atmospheric	0.5082 ± 0.0226	0.4643 ± 0.0192	1.0944 ± 0.0069	13.7 ± 3.7
PA6 / Low	0.5256 ± 0.0049	0.4725 ± 0.0106	1.1126 ± 0.0165	6.1 ± 2.5

Investigations of how printing conditions influenced surface energy, chemical functionality, as well as the thermal properties of the polymer layers were carried out. The results of the static water contact angle and surface energy measurements are given in Table 3. The polar component, for each of the printed polymers, decreases when printed under low pressure. This is most evident in the case of the PLA and PA6 printed polymers and may be due to the lack of oxygen present under the low-pressure printing conditions. The surface energies of the ABS and PLA polymers correlate well with values in the literature between 30 – 40 MJ/m^2 [24, 25]. The surface energy of 58 mJ/m^2, obtained for the PA6, when printed under atmospheric conditions however, is significantly higher than the literature value 35 mJ/m^2 [26]. Polyamides are hygroscopic and due to the hydrophilic character of the amide groups they are known to absorb water from their surroundings [22, 27]. The high surface energy obtained may be attributed with water absorption of the PA6 while printing. As detailed later in this paper, printing studies were also carried out under a nitrogen atmosphere. It is interesting to note that the surface energy of the PA6 decreased from the 58 MJ/m^2 in air to 40 MJ/m^2 under nitrogen, indicating decreased moisture adsorption under the controlled nitrogen atmosphere printing conditions.

Table 3: Water contact angle and surface energy of PME printed ABS, PLA and PA6 under both atmospheric and low-pressure conditions

Polymer / Pressure	WCA (°)	SE (MJ/m^2)	Polar (MJ/m^2)	Disp. (MJ/m^2)
ABS / Atmospheric	86 ± 3.1	39 ± 0.6	2 ± 0.8	37 ± 0.9
ABS / Low	86 ± 2.8	37 ± 0.3	1 ± 0.5	36 ± 0.7
PLA / Atmospheric	66 ± 7.0	39 ± 5.1	10 ± 2.0	30 ± 4.4
PLA / Low	85 ± 3.6	41 ± 0.9	2 ± 0.6	39 ± 0.4

PA6 / Atmospheric	36 ± 2.9	58 ± 1.3	23 ± 1.8	35 ± 2.2
PA6 / Low	80 ± 5.0	32 ± 0.5	11 ± 4.2	21 ± 4.6

3.2 Thermal and FT-IR Analysis

The thermal behaviour of the three polymers printed under both atmospheric and low-pressure conditions were investigated using DSC. Table 4 details the glass transition temperatures (T_g), the melting peak (T_m), the melting enthalpy (ΔH_m) and the percentage crystallinity (X_m), calculated using equation 2.

ABS is an amorphous polymer consisting of acrylonitrile, 1,3-butadiene and styrene. The first glass transition temperature, which ranged from -79 to -83°C is attributed to the poly-butadiene component [21]. In atmospheric conditions, the glass transition temperature decreases by 3°C, between the first and second heating cycle. A similar trend was observed for the ABS printed under low-pressure conditions. The second glass transition temperature obtained for ABS ranged between 103 and 105°C and is attributed to the acrylonitrile-styrene mesophase [21]. The use of low pressure printing conditions does not seem to have had an effect on the thermal stability of the ABS polymer.

The thermal behaviour of PLA, printed under both atmospheric and low-pressure conditions is detailed in Table 4. A large glass transition step at 61 and 62°C (second heating) was observed for the PLA printed under atmospheric and low-pressure conditions respectively, indicating a high percentage of amorphous material. A broad melting peak at 154°C (first heating) was observed for both printing conditions, which followed a broad post-crystallisation peak observed at 125°C, further indicating the amorphous nature of the printed PLA, as seen in Figure 6. Taking both peaks into consideration, the percentage crystallinity was calculated as 1% and 2% when printed under atmospheric and low-pressure respectively. It is thought that during the PME process, the PLA is cooled too fast to re-crystallise. It is concluded from this study that the effect of low-pressure printing conditions did not significantly change the thermal behaviour of the printed PLA.

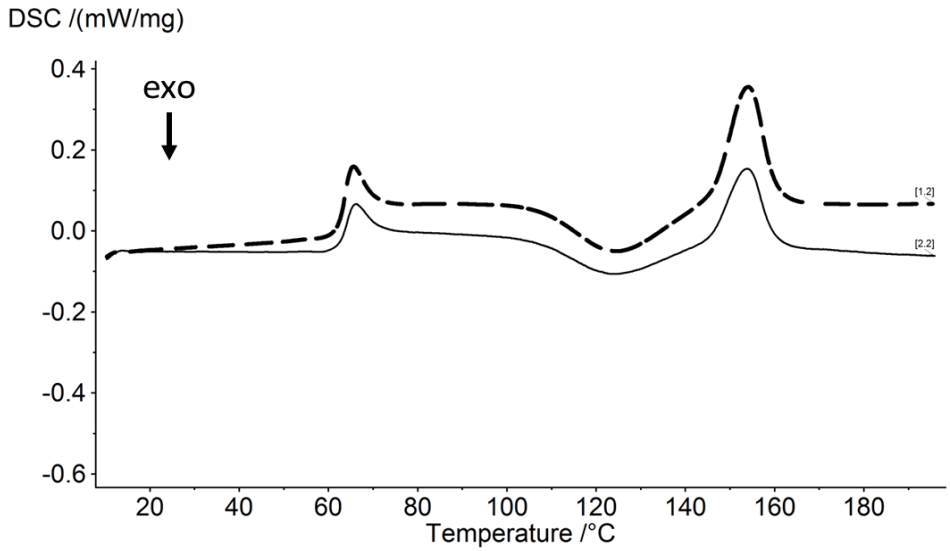

Figure 6: First heating cycle of PLA printed under atmospheric (top – dotted line) and low-pressure (bottom – black line), exhibiting a broad post-crystallisation peak at 125°C and broad melting peak at 154°C.

PA6 is a semi-crystalline polymer. Similar to PLA, the effect of low-pressure processing conditions does not influence its crystallinity. The DSC analysis reveals a broad peak in the first heating at 122°C, in PA6 printed under both conditions, likely due to the evaporation of water (Figure 7), which is also responsible for the significant shift in the glass transition temperatures when comparing the first and second heating cycles, under both printing conditions. The moisture peak exhibits an enthalpy of 28.12 J/g under atmospheric conditions and 16.32 J/g when printed under low pressure conditions, indicates a higher degree of water absorption in the printed PA6 polymer under atmospheric conditions. This is supported by the conclusions of the surface energy examination, detailed earlier.

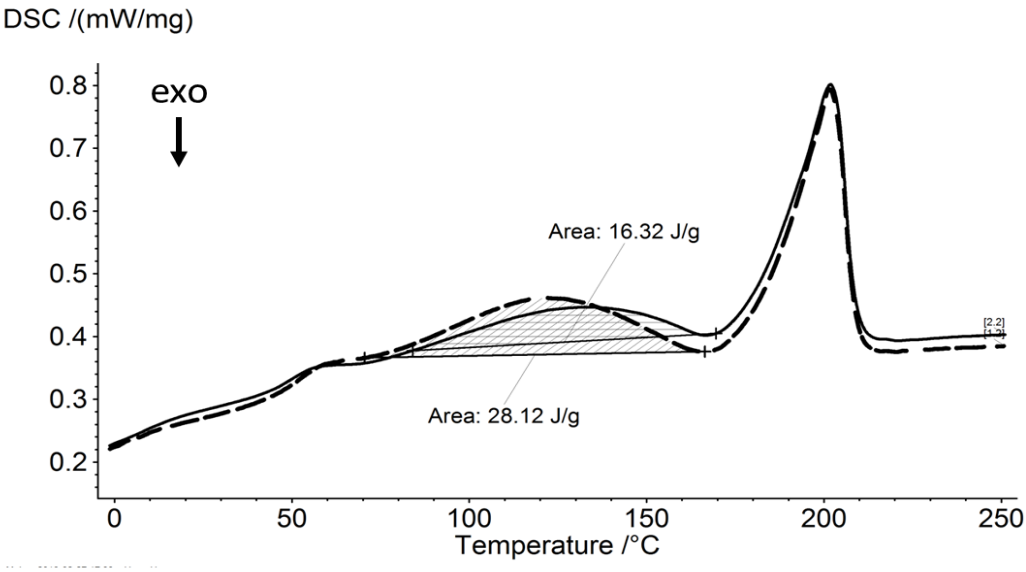

Figure 7: First heating cycles of PA6, printed under atmospheric (top – dotted line) and low pressure (bottom – black) exhibiting a broad peak attributed to moisture evaporation.

Table 4: Glass transition temperatures (T_g), the melting peak (T_m), the melting enthalpy (ΔH_m) and the percentage crystallinity (X_m) of printed ABS, PLA and PA6, under both atmospheric and low-pressure conditions.

Polymer / Printing Condition	**Heating Cycle**	**Tg (°C)**	**Tm (°C)**	**ΔHm (J/g)**	**Xm (%)**
ABS / Atmospheric	1st	-80, 103	-	-	-
	2nd	-83, 104	-	-	-
ABS / Low	1st	-79, 104	-	-	-
	2nd	-83, 105	-	-	-
PLA / Atmospheric	1st	63	154	15	1
	2nd	61	152	15	1
PLA / Low	1st	63	154	10	2
	2nd	62	153	10	1
PA6 / Atmospheric	1st	52	202	42	24
	2nd	46	200	39	22
PA6 / Low	1st	51	202	43	24
	2nd	45	200	37	21

ATR FT-IR analysis was also used to compare the three polymers printed under both atmospheric and low pressure. Figure 8 overlays the spectra of PLA, PA6 and ABS printed under atmospheric (solid line) and low-pressure (dotted line) conditions. Peaks characteristic of PLA at 2829 and 2932 cm^{-1}, 1748 cm^{-1}, 1082 cm^{-1} correspond to carbon to hydrogen stretching vibrations, the carbonyl group, and the carbon to oxygen to carbon stretching, respectively [7]. In the case of PA6, the peaks obtained at

3296 cm^{-1}, 1634 cm^{-1} and 1541 cm^{-1} correspond to the nitrogen to hydrogen stretching, the carbonyl group present in the amide and nitrogen to hydrogen bending, respectively [28]. The spectra of ABS exhibit characteristic peaks such as 700, 760, 1015, 1493 and 1601 cm^{-1} attributed to styrene and 911 and 966 cm^{-1} attributed to butadiene [21]. As expected, no significant spectral changes were observed the polymers printed under both conditions and it was concluded that no changes in the chemical functionality occurred between the polymers printed under both pressure regimes.

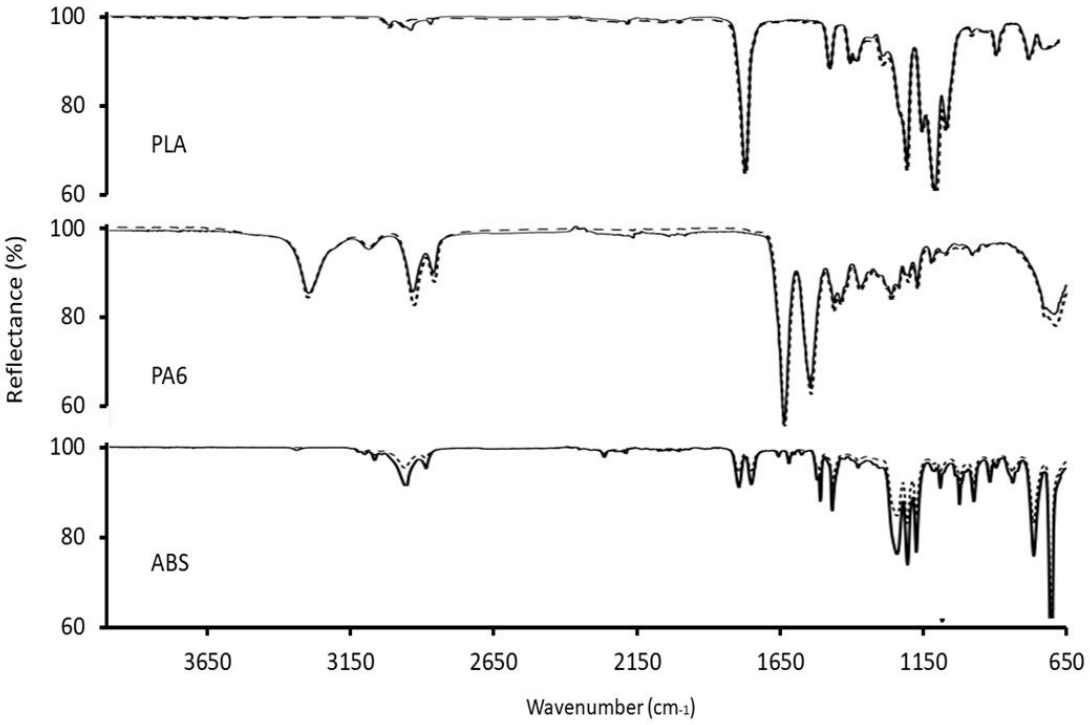

Figure 8: ATR-IR spectra of PLA, PA6 and ABS printed under atmospheric (solid line) and low-pressure (dotted line).

3.3 Mechanical Performance

The ultimate tensile strength (UTS), tensile modulus and the percentage elongation at break (ε_b) of the three polymers printed under both low and atmospheric pressure were compared. As shown in Table 5, low pressure printing conditions yielded a significant increase in the UTS for all three polymers, when compared to that obtained at atmospheric pressure.

ABS has been engineered with a high impact resistance and toughness and one of the most commonly used filaments for PME. The tensile properties of printed ABS have been widely reported and are typically in the range of 20 – 35 MPa, depending on the ABS material, printer and print parameters [8-10, 29, 30]. In this study, the ABS samples printed under atmospheric conditions yielded tensile strength

values of 34.2 MPa, while under low pressure processing conditions this increase by 9 % to 38.9 MPa. Low pressure processing conditions yielded a significant increase on the percentage elongation at break and a lower tensile modulus was observed. Cross section analysis of the ABS tensile specimen, given in Figure 11, compares both processing conditions. Under atmospheric pressure, the extruded polymer tracks are pulled until yielding, with necking and material separation evident between the layers. In comparison, under low pressure, no material separation is observed.

PLA is a widely used as filament for PME due to its low cost and excellent mechanical properties. The tensile strength of printed PLA typically ranges between 35 – 55 MPa depending on the filament purity, printer and print parameters chosen [31-33]. As demonstrated in Table 5 there was a 14% increase in tensile strength when comparing atmospheric with low-pressure printing conditions. The PLA failure modes were identical under both atmospheric and low-pressure printing, however a reduction in the print porosity and an enhanced layer to layer adhesion is evident from the cross-sectional analysis of the tensile specimen, given in Figure 11. Similar to that observed for the ABS, the elongation of the tensile specimen increased and the tensile modulus decreased when fabricated under low-pressure conditions (Figure 9).

PA6 is used in many structural applications due to its characteristically high strength, stiffness and chemical resistance. Under low-pressure processing conditions the PA6 exhibited the highest increase in UTS of 42%. The percentage elongation of the polymer did not change significantly when printed under both conditions. The tensile modulus however, increased when printed under low-pressure, suggesting the low-pressure processing yielded a less elastic print. The mechanical strength of printed polymeric parts is highly sensitive to the degree of molecular diffusion achieved at the interface of the deposited layers [3] and this molecular diffusion is thermally driven. It is likely that the PA6 specimens experienced the highest level of molecular diffusion, in comparison to the ABS and PLA polymers, as it characteristically has a lower glass transition and melting temperature [22], hence yielding the highest increase in UTS. These specimens exhibited a more ductile failure overall, when compared to the other two polymers, typical of polyamides, given in Figure 10.

Table 5: Ultimate tensile strength, percentage elongation at break (εb) and tensile modulus of the three polymers printed under both atmospheric and low-pressure conditions.

Polymer / Pressure	**UTS (MPa)**	**Elongation at Break, ε_b (%)**	**Tensile Modulus, E_t (MPa)**
ABS / Atmospheric	34.2 ± 1.2	2.8 ± 0.1	1624.3 ± 59.5
ABS / Low	38.9 ± 0.9	5.2 ± 1.9	1402.3 ± 78.0
PLA / Atmospheric	56.5 ± 2.4	3.4 ± 0.1	1847.1 ± 34.2
PLA / Low	63.7 ± 1.9	4.2 ± 0.2	1783.5 ± 32.4
PA6 / Atmospheric	42.8 ± 6.7	88.5 ± 30.4	1257.3 ± 65.5
PA6 / Low	60.6 ± 12.0	91.2 ± 12.5	1695.1 ± 101.1
PA6 / Nitrogen	45.5 ± 7.0	88.4 ± 23.2	1207.6 ± 176.4

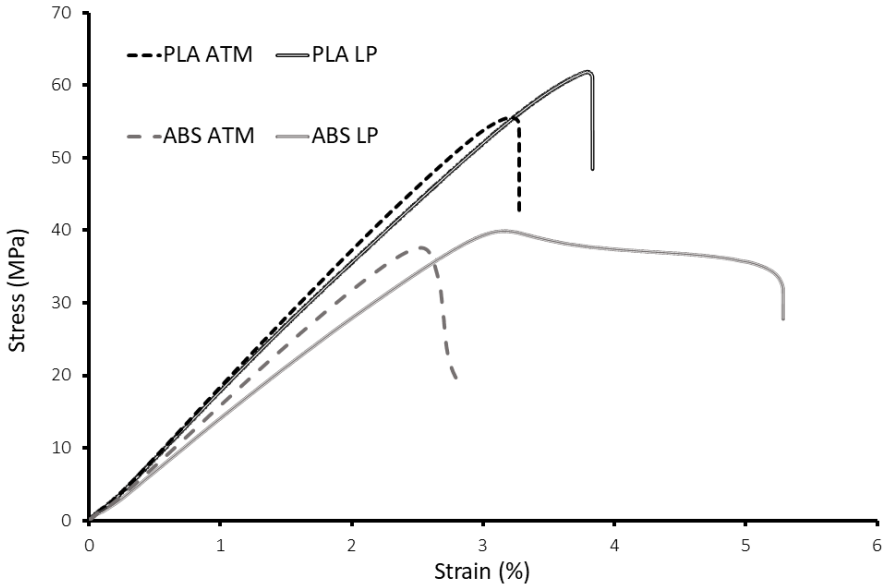

Figure 9: An example of stress strain curves, typical for that of ABS and PLA tensile specimen at both atmospheric (dotted line) and low-pressure (solid line) conditions.

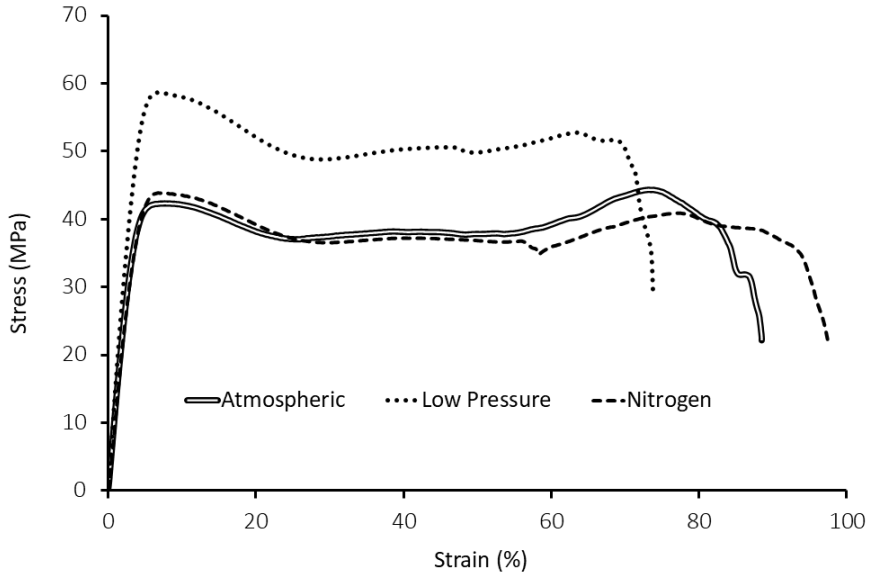

Figure 10: An example of a typical stress strain curves obtained for the PA6 printed polymer, under the atmospheric, low pressure and nitrogen atmosphere.

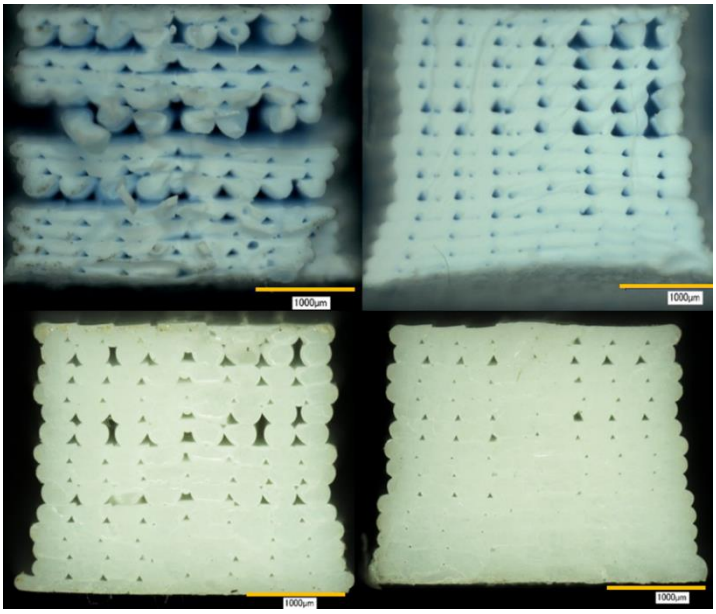

Figure 11: Cross section examination of the tensile fracture area ABS (top) and PLA (bottom) - printed under atmospheric pressure (left) and low pressure (right). Scale bar 1000 µm.

3.4 Printing Under Nitrogen

In the study to date, it was shown that low-pressure printing yielded enhanced mechanical performance. It was previously reported that, removing oxygen from the PME printing atmosphere, may prevent oxidation of the deposited nylon co-polymer layer and in turn enhance its tensile strength [12]. This study reported an increase in UTS of almost 30 % when nylon co-polymer was printed in a N_2 glovebox. It was proposed that the increased mechanical performance was associated with reduced oxidation of the filament and thus enhanced bonding between the filaments. An investigation was carried out in order to determine if the reason for the enhanced mechanical performance obtained at low-pressure in this current study was due to the lack of oxygen on PME printed parts. A study was carried out which involved printing with PA6 in a low oxygen environment. This was achieved by firstly placing the printer in the vacuum chamber and evacuation to 1 Pa as before. The chamber was then brought up to atmospheric pressure by backfilling with N_2 gas. During printing, a constant nitrogen purge was maintained on the chamber. The results of this study are presented in Figures 12 and 13. The UTS of the PA6 polymer printed under atmospheric pressure and under nitrogen are close in value. Similarly, the tensile modulus of the polymer, printed under atmospheric pressure and under nitrogen yielded almost identical values. The error of the PA6 however, printed under nitrogen, increased when compared to that of the PA6 printed under atmospheric conditions, thus showing a larger variation in the modulus. It was demonstrated from this study, that the PA6 printed under nitrogen exhibited tensile results similar to those obtained for the PA6 printed at atmospheric pressure. Thus, the exclusion of oxygen during printing did not significantly influence the mechanical performance of this polymer.

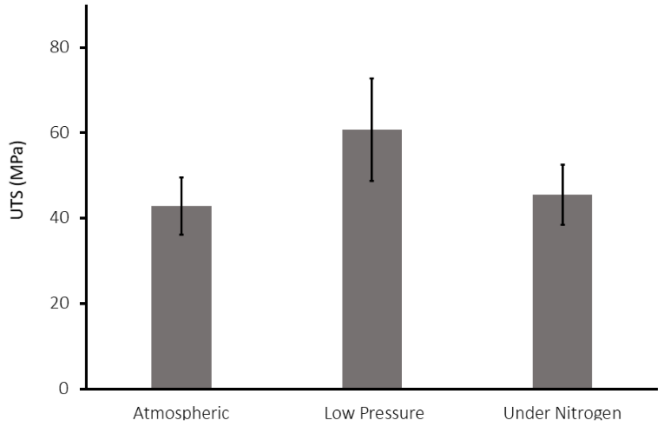

Figure 12: UTS of PA6 test samples printed under atmospheric, low pressure and nitrogen atmosphere.

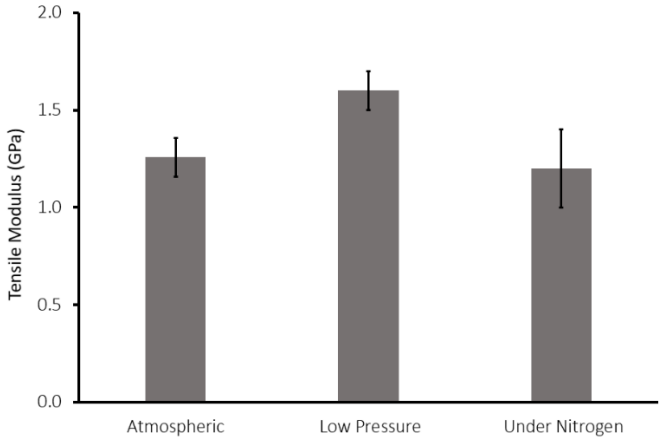

Figure 13: Tensile Modulus of PA6 printed under atmospheric, low pressure and nitrogen atmosphere.

The enhanced mechanical strength obtained for parts printed under reduced pressure is likely to be due to a combination of factors. Firstly, the reduction in porosity, evident in the printed specimen under low pressure (Figure 11, 14) could enhance the layer to layer adhesion, which in turn increases the UTS. The increase in average mass, volume and density of the printed coupons (Table 2) also give a clear indication and comparison of the level of porosity present in the samples. The second factor, likely to be enhancing the mechanical performance of the polymers printed under low pressure, is the reduction of residual stresses. It has been widely reported that, under standard atmospheric pressure, residual stresses accumulate due to the repetitive heating and cooling cycle of the polymer during the PME process [6, 34, 35]. The heating and rapid cooling cycle results in non-uniform thermal gradient and a build-up of stress. Under low-pressure processing conditions, the fabricated parts are not subject to the

same thermal gradient or cooling cycle as much less heat is dissipated and the printed specimens are unable to fully cool. Furthermore, the reduction in cooling of the print that occurs when printed under low pressure, may allow enhanced bonding of the layers through thermally driven molecular diffusion of the polymer, enhancing the tensile strength of the print.

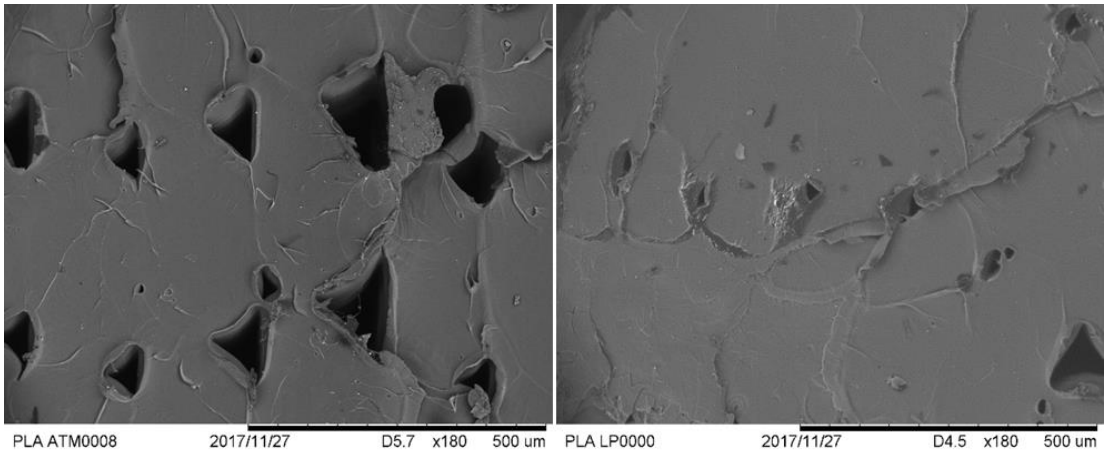

Figure 14: SEM micrographs of PME fabricated PLA under atmospheric conditions (left) and low pressure (right), showing reduced size of air gaps / porosity when printing under low pressure.

4. Conclusion

Acrylonitrile butadiene styrene (ABS), polylactic acid (PLA) and polyamide 6 (PA6) were fabricated via polymer material extrusion (PME), under atmospheric and under low pressure conditions (1Pa), and the effect on their mechanical and physical properties investigated.

Under low pressure conditions, the printed coupons exhibited a higher mass, volume, density and lower porosity. The low-pressure coupons also exhibited a higher surface finish, with the individual print tracks being less defined. Chemical functionality and thermal properties of the printed polymers were similar for these polymers printed under the two pressure regimes. DSC analysis suggested a higher degree of water absorption occurring when PA6 is printed under atmospheric conditions. The surface energy of the printed polymers exhibited a decrease in polar component under low pressure, compared with atmospheric conditions. This may be associated with a reduction in oxygen functionality on the polymer surface.

The low-pressure printing conditions increased the UTS of ABS, PLA and PA6 by 9, 13 and 42% respectively, when compared to atmospheric conditions. The percentage elongation at break for the PLA and ABS saw a significant increase as the tensile modulus decreased, indicating the PLA and ABS polymer becomes more ductile when printed under low-pressure conditions. Based on a print study carried out with PA6 under a nitrogen atmosphere, it was concluded that the prevention of oxidation was not the explanation for the enhanced mechanical performance obtained with low pressure printing. Possible reasons for this enhanced performance are:

- Superior bonding between the deposited polymer layers due to a reduction in temperature gradient.
- A reduction in the accumulation of stress, as the typical rapid heating and cooling cycle, of the PME process is reduced.
- Enhanced layer to layer adhesion due to the reduction in air gaps / porosity of the prints.

Acknowledgements:

This work was supported under both the MaREI SFI Centre for Marine Renewable Energy Research - (12/RC/2302) and the IForm Advanced Manufacturing Reseach Centre - (16/RC/3872). The IR spectral acquisition was supported by the European Commission under the 7th Framework Programme (Grant agreement no:335508).

References

[1] O.A. Mohamed, S.H. Masood, J.L. Bhowmik, Optimization of fused deposition modeling process parameters: a review of current research and future prospects, Advances in Manufacturing 3(1) (2015) 42-53.
[2] K.V. Wong, A. Hernandez, A Review of Additive Manufacturing, ISRN Mechanical Engineering 2012 (2012) 1-10.
[3] G.M.R. Q. Sun, C.T. Bellehumeur and P. Gu, Effect of processing conditions on the bonding quality of FDM polymer filaments, Rapid Prototyping Journal 14(2) (2008) 72 - 80.
[4] D.R.R. T. Nancharaiah, V. R. R., An experimental investigation on surface quality and dimensional accuracy of FDM components, International Journal on Emerging Technologies 1(2) (2010) 106 - 111.
[5] A.K. Sood, R.K. Ohdar, S.S. Mahapatra, Improving dimensional accuracy of Fused Deposition Modelling processed part using grey Taguchi method, Materials & Design 30(10) (2009) 4243-4252.
[6] Y. Zhang, K. Chou, A parametric study of part distortions in fused deposition modelling using three-dimensional finite element analysis, Proceedings of the Institution of Mechanical Engineers, Part B: Journal of Engineering Manufacture 222(8) (2008) 959-968.
[7] A. Lanzotti, D. Eujin Pei, M. Grasso, G. Staiano, M. Martorelli, The impact of process parameters on mechanical properties of parts fabricated in PLA with an open-source 3-D printer, Rapid Prototyping Journal 21(5) (2015) 604-617.
[8] J.F. Rodríguez, J.P. Thomas, J.E. Renaud, Mechanical behavior of acrylonitrile butadiene styrene fused deposition materials modeling, Rapid Prototyping Journal 9(4) (2003) 219-230.
[9] S. Ziemian, M. Okwara, C.W. Ziemian, Tensile and fatigue behavior of layered acrylonitrile butadiene styrene, Rapid Prototyping Journal 21(3) (2015) 270-278.
[10] O.S. Es-Said, J. Foyos, R. Noorani, M. Mendelson, R. Marloth, B.A. Pregger, Effect of Layer Orientation on Mechanical Properties of Rapid Prototyped Samples, Materials and Manufacturing Processes 15(1) (2000) 107-122.
[11] N.G. Tanikella, B. Wittbrodt, J.M. Pearce, Tensile strength of commercial polymer materials for fused filament fabrication 3D printing, Additive Manufacturing 15 (2017) 40-47.
[12] F. Lederle, F. Meyer, G.-P. Brunotte, C. Kaldun, E.G. Hübner, Improved mechanical properties of 3D-printed parts by fused deposition modeling processed under the exclusion of oxygen, Progress in Additive Manufacturing 1(1-2) (2016) 3-7.
[13] Ultimaker, Ultimaker Cura 3D Printing Software. (Accessed 1/10/17 2017).
[14] A. Kantaros, D. Karalekas, FBG Based In Situ Characterization of Residual Strains in FDM Process, (2014) 333-337.
[15] S.W. Hughes, Archimedes revisited: a faster, better, cheaper method of accurately measuring the volume of small objects, Physics Education 40(5) (2005) 468 - 474.
[16] J.N.H. Y.Kong, The measurement of the crystallinity of polymers by DSC, Polymer 43 (2002) 3873 - 3878.
[17] D. Garlotta, A Literature Review of Poly(Lactic Acid), Journal of Polymers and the Envirnment 9(2) (2001) 63 - 80.
[18] T.K. V.P.Privalko, Yu.S.Lipatov, Crystallization of Filled Nylon 6. I. Heat Capacities and Melting Behavior Polymer Journal 11(9) (1979) 699 - 709
[19] R.C.W. D. K. Owens, Estimation of the Surface Free Energy of Polymers, Journal of Applied Polymer Science 13(8) (1969) 1741 - 1747.
[20] A. International, Standard Test Method for Tensile Properties of Plastics, ASTM D 638 - 02a (2002).
[21] G. Wypych, ABS poly(acrylonitrile-co-butadiene-co-styrene), Hanbook of Polymers, Elsevier2012, pp. 3 - 10.
[22] Polymer Data Handbook, Oxford University Press1999.
[23] Markforged, Material Spec - Nylon PA6, 2017. (Accessed 1/10/17 2017).
[24] V. Khoshkava, M.R. Kamal, Effect of surface energy on dispersion and mechanical properties of polymer/nanocrystalline cellulose nanocomposites, Biomacromolecules 14(9) (2013) 3155-63.
[25] D. Enterprises, Surface Energy Data for ABS: Acrylonitrile butadiene styrene, 2009. (Accessed 27/11/17 2017).

[26] M. Noeske, J. Degenhardt, S. Strudthoff, U. Lommatzsch, Plasma jet treatment of five polymers at atmospheric pressure: surface modifications and the relevance for adhesion, International Journal of Adhesion and Adhesives 24(2) (2004) 171-177.
[27] W. Michaeli, F. von Fragstein, K. Bahroun, H. Behm, C. Hopmann, Investigations on the influence of hygroscopic surfaces on the plasma-assisted modification of polyamide, Surface and Coatings Technology 205 (2011) S506-S510.
[28] H.I. G. Rotter, FTIR Separation of Nylon-6 Chain Conformations: Clarification of the Mesomorphous and y-Crystalline Phases, Journal of Polymer Science: Part B: Polymer Physics 30 (1992) 489 - 495
[29] S.H. Ahn, M. Montero, D. Odell, S. Roundy, P.K. Wright, Anisotropic material properties of fused deposition modeling ABS, Rapid Prototyping Journal 8(4) (2002) 248-257.
[30] M. Dawoud, I. Taha, S.J. Ebeid, Mechanical behaviour of ABS: An experimental study using FDM and injection moulding techniques, Journal of Manufacturing Processes 21 (2016) 39-45.
[31] M.F. Afrose, S.H. Masood, M. Nikzad, P. Iovenitti, Effects of Build Orientations on Tensile Properties of PLA Material Processed by FDM, Advanced Materials Research 1044-1045 (2014) 31-34.
[32] B. Wittbrodt, J.M. Pearce, The effects of PLA color on material properties of 3-D printed components, Additive Manufacturing 8 (2015) 110-116.
[33] J. Torres, J. Cotelo, J. Karl, A.P. Gordon, Mechanical Property Optimization of FDM PLA in Shear with Multiple Objectives, Jom 67(5) (2015) 1183-1193.
[34] C. Casavola, A. Cazzato, V. Moramarco, G. Pappalettera, Residual stress measurement in Fused Deposition Modelling parts, Polymer Testing 58 (2017) 249-255.
[35] A.K. Sood, R.K. Ohdar, S.S. Mahapatra, Parametric appraisal of mechanical property of fused deposition modelling processed parts, Materials & Design 31(1) (2010) 287-295.